Inorganica Chimica Acta, 196 (1992) 231–240

Bonding properties of Cu(II)–imidazole chromophores: spectroscopic and electrochemical properties of monosubstituted imidazole copper(II) complexes. Molecular structure of [Cu(4-methylimidazole)$_4$(ClO$_4$)$_2$]

Chan-Cheng Su*, Jan Hua Chen, Kuo-Yih Hwang, Shyh-Jiun Liu, Shion-Wen Wang
Department of Chemistry, National Taiwan Normal University, Taipei (Taiwan)

Sue-Lein Wang and Sheng-Nan Liu
Department of Chemistry, National Tsing Hua University, Hsinchu (Taiwan)

(Received January 27, 1992; revised April 4, 1992)

Abstract

The synthesis, electronic, vibrational and EPR spectra, and cyclic voltammetry are reported for methylimidazoles and *N*-acetylhistamine copper(II) complexes. The crystal and molecular structure of [Cu(4-methylimidazole)$_4$(ClO$_4$)$_2$] has been determined using three-dimensional X-ray diffraction data. The complex crystallizes in the monoclinic space group *C2/c* with $a=15.742(5)$, $b=10.052(3)$, $c=16.654(5)$ Å, $\beta=111.81(2)°$, and $Z=4$. Least-squares refinement of the structure gave a final R factor of 0.0454 and $R_w=0.0450$ for 1284 independent reflections. The structure consists of discrete centrosymmetric [Cu(4-methylimidazole)$_4$(ClO$_4$)$_2$] units interconnected by hydrogen bonds, having a CuN$_4$ plane with Cu–N distances of 1.993(4) and 2.007(5) Å and two perchlorates on the long z axis with Cu–O of 2.659(4) Å. The dihedral angles between the imidazole and the CuN$_4$ planes are 79.3 and 105.6°. The properties of the copper(II)–imidazole bonds are analyzed with reference to the electronic structures of the tetrakis(monosubstituted imidazole)-copper(II) complexes having effective local symmetry of D_{4h} or D_{2h}. The Cu(II) ion can accommodate at most four imidazole ligands for *N*-acetylhistamine and 2-methylimidazole, but upto six for 4-methylimidazole, *N*-methylimidazole and imidazole. In acetonitrile solution, the reduction potentials for the tetragonal copper(II) complexes containing four imidazole ligands parallel the pK_a values of the imidazole ligands. This may be ascribed to the enhanced stabilities of Cu(I) complexes by the σ-donor abilities of the imidazole ligands.

Introduction

The widely observed interactions of the copper–histidyl residue of proteins [1] have prompted a considerable number of research activities dealing with the properties of copper–imidazole compounds of low molecular weights [2]. Results of these studies have shed light on our understanding of the copper–imidazole bonding. Since the histidyl residue has a substituent group linked at the 4-position of the imidazole nucleus, on which electronic effects and perhaps steric congestion may impose, the bonding properties of the copper–imidazole chromophores are, therefore, expected to be influenced. In our recent studies on tetrakis(imidazole)copper(II) complexes [3], we have found that the dihedral angles between the imidazole and the CuN$_4$ planes are altered either by changing the axial anions or upon formation of hydrogen bonds on imidazole N–H groups. Accordingly, changes in the bonding capabilities of the imidazole ligands have been suggested to account for the stereochemistry of the tetrakis(imidazole)copper(II) complexes. In this connection investigation on 4-substituted imidazole copper(II) complexes should render results on the bonding properties of Cu–imidazole more closely related to the copper–histidyl interactions. Here, we report the molecular structure of the title complex and the spectral and electrochemical behavior and bonding properties of monosubstituted imidazole copper(II) complexes.

*Author to whom correspondence should be addressed.

Experimental

Materials

4-Methylimidazole (Aldrich), 2-methylimidazole (Merck), *N*-methylimidazole (Merck), *N*-acetylhis-

0020-1693/92/$5.00

tamine (Aldrich), imidazole (Merck), 2,2-dimethoxypropane (Sigma), $CuCl_2 \cdot 2H_2O$ (Wako), $NaClO_4$ (Cica), $Cu(NO_3)_2 \cdot 3H_2O$ (Wako) and organic solvents of reagent grade and spectrograde were used as received. Anhydrous CH_3CN for cyclic voltammetry measurements was obtained by refluxing over and then distilling off P_4O_{10}. The supporting electrolyte, $(C_2H_5)_4NBF_4$ (Merck), was dried over P_4O_{10} before use. Anhydrous $Cu(BF_4)_2$ was prepared from CuO and HBF_4 and dried *in vacuo* over P_4O_{10} at 100 °C. $[Cu(4MImH)_4Cl_2]$ [4], $[Cu(4MImH)_4(NO_3)_2]$ [4] and $[Cu(ImH)_4Cl_2]$ [5] were prepared according to the cited literature. (For abbreviations see footnote of Table 4, p. xxx.)

Preparations

Cu(4-methylimidazole)$_4$(ClO$_4$)$_2$

To 1.0 ml of 1.0 M aqueous $CuCl_2 \cdot 2H_2O$ (0.171 g) solution, 7.0 ml of 1.0 M aqueous 4-methylimidazole (0.575 g) solution were added dropwise. The solution was heated in a water bath for 20 min and then a 0.1 M HCl solution was added dropwise until the gray precipitates completely disappeared. Then 1.0 ml of 4.0 M aqueous $NaClO_4$ solution was added, and the clear solution was stored overnight. Purple crystals suitable for X-ray diffraction work were obtained. Yield 83%; m.p. 198 °C (dec.) *Anal.* Found: C, 32.6; H, 3.85; N, 19.0. Calc. for $C_{16}H_{24}N_8O_8Cl_2Cu$: C, 32.49; H, 4.06; N, 18.95%.

Cu(N-methylimidazole)$_4$(ClO$_4$)$_2$

To 1.0 ml of 1.0 M aqueous $CuCl_2 \cdot 2H_2O$ (0.171 g) solution, 6.0 ml of 1.0 M aqueous *N*-methylimidazole (0.493 g) solution were added dropwise. The solution was heated in a water bath for 10 min and then 1 ml of 3.0 M aqueous $NaClO_4$ solution was slowly added. The clear solution was stored overnight. Bluish purple crystalline products were obtained. Yield 79%, m.p.

TABLE 1. Summary of crystal data and intensity collection

Empirical formula	$CuC_{16}H_{24}N_8Cl_2O_8$
Color; habit	purple; chunk
Crystal size (mm)	$0.30 \times 0.15 \times 0.15$
Space group	$C2/c$; monoclinic
Unit cell dimensions	
a (Å)	15.742(5)
b (Å)	10.052(3)
c (Å)	16.654(5)
β (°)	111.81(2)
Volume (Å^3)	2446.8(13)
Z	4
Formula weight	590.9
Density (calc.) (Mg/m^3)	1.604
Absorption coefficient (mm^{-1})	1.169
F(000)	1212
Diffractometer used	Siemens R3m/V
Radiation	Mo Kα ($\lambda = 0.71073$ Å)
Temperature (K)	297
Monochromator	highly oriented graphite crystal
2θ range (°)	2.5–45.0
Scan type	$\theta/2\theta$
Scan speed (°/min)	variable; 2.93–14.65 in ω
Scan range (ω)	1.06° plus Kα separation
Background measurement	stationary crystal and stationary counter at beginning and end of scan, each for 25.0% of total scan time
Standard reflections	3 measured every 50 reflections
Index ranges	$-18 \leqslant h \leqslant 0$, $0 \leqslant k \leqslant 10$, $-18 \leqslant l \leqslant 19$
Reflections collected	3575 ($1584 > 3.0\sigma(I)$)
Independent reflections	1830 ($1284 > 3.0\sigma(I)$)
Extinction correction	$\chi = 0.00001(10)$, where $F^* = F[1 + 0.002\chi F^2/\sin(2\theta)]^{-1/4}$
Weighting scheme	$w^{-1} = \sigma^2(F) + 0.0005F^2$
No. parameters refined	177
Final R indices (obs. data)	$R = 0.0454$, $R_w = 0.0450$
Goodness-of-fit	0.95
Largest and mean Δ/σ	0.020, 0.001
Data-to-parameter ratio	7.3:1
Largest difference peak (e Å^{-3})	0.57
Largest difference hole (e Å^{-3})	−0.37

242 °C (dec.) *Anal.* Found: C, 32,2; H, 3.82; N, 18.9. Calc. for $C_{16}H_{24}N_8O_8Cl_2Cu$: C, 32.49; H, 4.06; N, 18.95%.

Cu(2-methylimidazole)$_3$(H$_2$O)$_2$(ClO$_4$)$_2$

To an aqueous solution of 0.371 g (1 mmol) $Cu(ClO_4)_2 \cdot 6H_2O$, an aqueous solution of 0.328 g (4 mmol) 2-methylimidazole was added slowly. The blue solution was stirred for 10 min. Blue precipitates were filtered off and dried *in vacuo* over P_4O_{10}. Yield 46%; m.p. 141 °C (dec.) *Anal.* Found: C, 26.2; H, 3.83; N, 15.2. Calc. for $C_{12}H_{22}N_6O_{10}Cl_2Cu$: C, 26.4; H, 4.04; N, 15.4%.

Cu(N-acetylhistamine)$_4$Cl$_2$

An ethanol solution consisting of 0.0538 g of $CuCl_2 \cdot 2H_2O$ (0.316 mmol) and 0.245 g of *N*-acetylhistamine (1.6 mmol) was stirred for 1 h. Acetone was added until the solution became turbid. After storing in a refrigerator overnight, the bluish purple products were filtered off and recrystallized from CH_3OH and CH_3CN, and then dried over P_4O_{10} *in vacuo*. Yield 78%; m.p. 168–172 °C. *Anal.* Found: C, 44.6; H, 5.58; N, 22.0. Calc. for $C_{28}H_{44}N_{12}O_4Cl_2Cu$: C, 44.85; H, 6.02; N, 22.02%.

Cu(N-acetylhistamine)$_2$(NO$_3$)$_2$

An ethanol solution consisting of 0.0966 g of $Cu(NO_3)_2 \cdot 3H_2O$ (0.4 mmol) and 0.123 g of *N*-acetylhistamine (0.8 mmol) was stirred at 65 °C for 5 h. The blue products were filtered off and recrystallized from CH_3OH and CH_3CN, and then dried over P_4O_{10} *in vacuo*. Yield 76%; m.p. 182 °C (dec.) *Anal.* Found: C, 34.1; H, 4.35; N, 22.7. Calc. for $C_{14}H_{22}N_8O_8Cu$: C, 34.0; H, 4.48; N, 22.68%.

Physical measurements

IR spectra were recorded as Nujol mulls or KBr pellets on a BIO-RAD FTS-40 FTIR. A Jasco model 7850 spectrophotometer was used for electronic spectra measurements. Spectra of solid samples were recorded as Nujol mulls on Whatman No. 1 filter paper. The deconvolution of solid visible spectra into Gaussian component bands was performed on a VAX 8530 computer using the profile-fitting program CUVFIT [6]. EPR spectra were obtained by using a Brucker ER 200D 10/12 model spectrometer and calibrated with DPPH ($g = 2.0037$). Elemental analyses were carried out by the microanalysis laboratories of Taiwan University, Taipei. Cyclic voltammograms were recorded utilizing a PAR-273 potentiostat equipped with an IBM PC. The three-electrode cell comprised an SCE reference electrode, a Pt auxiliary electrode and a glassy carbon working electrode. Ferrocene solutions were used as reference to calibrate the cyclic voltammetry scale and to assign the potential values not affected by the variable diffusion potential arising at the interface of the aqueous SCE. A Micro Vax II computer-controlled Siemens R3m/V diffractometer was used for crystal and molecular structure determination.

Structure determination and refinement

Details of crystal data and intensity collection are summarized in Table 1. Twelve independent reflections with $10.15 \leqslant 2\theta \leqslant 28.14°$ were used for least-squares determination of the cell constants. Diffractometer examination of the reciprocal lattice showed the space group to be *C*2/*c* from the following systematic absences: hkl, $h+k \neq 2n+1$; $h0l$, $l \neq 2n+1$. Intensity data ($\theta/2\theta$ scan, $2.5 \leqslant 2\theta \leqslant 45°$, $(\sin\theta/\lambda)_{max} \sim 0.538$) were collected at 297 K for two octants of the sphere ($-18 \leqslant h \leqslant 0$, $0 \leqslant k \leqslant 10$, $-18 \leqslant l \leqslant 19$) and corrected for Lorentz and polarization effects but not for absorption. Three standard reflections were monitored every 50 reflections and showed no signs of crystal deterioration. The structure was solved by direct methods using the SHELXTL PLUS program [7] and refined by full-matrix least-squares on *F* values. Scattering form factors and anomalous dispersion correction terms were taken from the International Tables for X-ray Crystallography [8]. The quantity minimized was $\Sigma w(KF_o - F_c)^2$, with weights w equal to $[\sigma^2(F_o) + gF_o^2]^{-1}$, where $g = 0.0005$. All hydrogen atoms included in the refinement were placed in idealized positions (C–H = 0.96 Å, H–C–H = 109.4°) after non-hydrogen atoms were refined anisotropically. All calculations were done on a Micro Vax II-based Nicolet SHELXTL PLUS system.

Results and discussion

The crystal and molecular structure of $[Cu(4MImH)_4(ClO_4)_2]$ is shown in Figs. 1 and 2. Bond lengths and bond angles are listed in Table 2. The atomic coordinates are given in Table 3. The copper ion is bound centrosymmetrically by six ligands forming an elongated octahedron with four 4-methylimidazole ligands in the *xy* plane, Cu–N 1.993(4) and 2.007(5) Å, and two perchlorates on the long *z* axis, Cu–O 2.659(4) Å. The central copper ion lies on the inversion center and the asymmetric unit consists of only half of the molecule. The discrete $[Cu(4MImH)_4(ClO_4)_2]$ complexes are interconnected by hydrogen bonds between imidazole N(2) and perchlorate O(4) of the neighboring complex and by bifurcated hydrogen bonds [9] between imidazole N(4) and perchlorate O(2) and a second perchlorate O(1) of the neighbouring complexes. Both imidazole units are oriented approximately perpendicular to the CuN_4 coordination plane; the dihedral angles between the best planes are 79.3 and 105.6°. The bond distances and angles of the 4-methylimidazole ligands

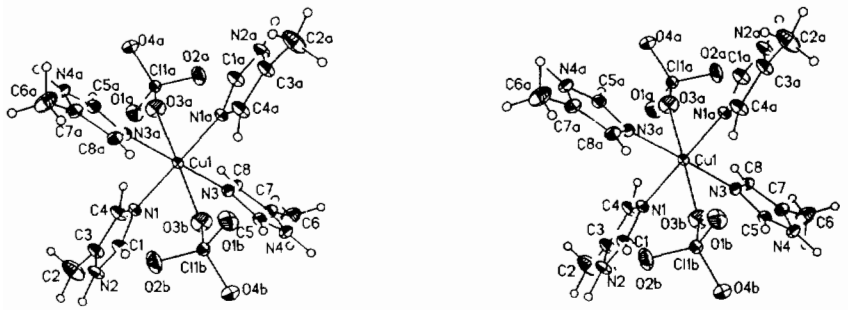

Fig. 1. Stereoscopic diagram of the copper coordination of $[Cu(4\text{-methylimidazole})_4(ClO_4)_2]$.

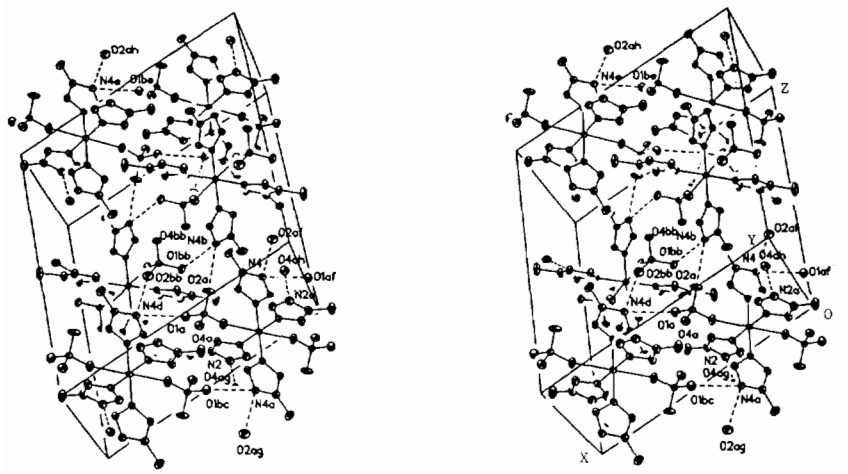

Fig. 2. Stereoscopic drawing of the molecular packing in the unit cell. Hydrogen bond, N2...O4, 2.980 Å; and bifurcated hydrogen bond, N4...O2, 2.965 Å and N4...O1, 3.208 Å.

and the loosely bound perchlorates are in the normal ranges.

The electronic, vibrational and EPR spectral data for the monosubstituted imidazole copper(II) complexes along with the relevant imidazole complexes are listed in Table 4. The solid state visible spectra of the tetrakis complexes can be categorized into two groups analogous to the previously reported tetrakisimidazole complexes [3]. The first group, consisting of 4-methylimidazole complexes, $[Cu(achmH)_4Cl_2]$ and $[Cu(ImH)_4(NO_3)_2]$, exhibits an absorption maximum of the LF bands at about 510–591 nm with a flanking shoulder at ~100 nm longer wavelength; the second group, including $[Cu(NMIm)_4(ClO_4)_2]$ and $[Cu(ImH)_4(ClO_4)_2]$, shows an asymmetric broad LF band at ~560 nm. The difference in spectral contour stems from the orientations of the bound imidazole ligands and consequently the bonding capabilities of the Cu–imidazole chromophores.

In order to reveal the correlation of the bonding abilities and the orientations of the coordinated imidazole nuclei, the solid state visible spectra of the tetrakis complexes were deconvoluted into Gaussian component bands by curve-fitting iteration processes. Each complex had an excellent fit with the reliability factor R^*, less than ~0.6% as illustrated in Fig. 3. The resultant peak positions are given in Table 5 together with their relative absorptivities and half-height widths. Three Gaussian component bands, with that of the highest frequency having the greatest intensity, were resolved for the first group complexes. The lowest energy component of these complexes showed very low peak intensity. A similar situation was observed in the single crystal polarized spectrum of the tetragonal $[Cu(ImH)_6](NO_3)_2$ [10]. The d orbitals were assigned in the sequence of $d_{x^2-y^2} > d_{z^2} > d_{xy} > d_{xz} = d_{yz}$, as the energy levels reported for the tetragonal CuN_4X_2 complexes [11]. The degeneracy of the d_{xz} and d_{yz} orbitals suggests that the complexes must contain CuN_4 chromophores with an effective D_{4h} symmetry, i.e. all four bound imidazole nuclei lie approximately perpendicular to the CuN_4 plane, like the structures of the title complex and $[Cu(ImH)_4(NO_3)_2]$ [12]. The complexes of the second group show four Gaussian component bands, corresponding to the sequence of d orbitals as $d_{x^2-y^2} > d_{z^2} > d_{xy} > d_{xz} > d_{yz}$. Here, the degeneracy of d_{xz} and d_{yz} orbitals is removed, because the CuN_4 chro-

*See footnote c, Table 5, p. 236.

TABLE 2. Bond lengths (Å) and bond angles (°)

Cu(1)–N(1)	1.993(4)	Cu(1)–N(3)	2.007(5)
Cl(1)–O(1)	1.410(5)	Cl(1)–O(2)	1.421(7)
Cl(1)–O(3)	1.431(5)	Cl(1)–O(4)	1.429(5)
N(1)–C(1)	1.382(7)	N(1)–C(4)	1.305(8)
N(2)–C(1)	1.332(10)	N(2)–C(2)	1.503(10)
N(2)–C(3)	1.345(8)	N(3)–C(5)	1.367(7)
N(3)–C(8)	1.320(9)	N(4)–C(5)	1.345(10)
N(4)–C(6)	1.488(9)	N(4)–C(7)	1.362(8)
C(3)–C(4)	1.331(8)	C(7)–C(8)	1.345(9)
Cu(1)–O(3)	2.659(4)		
N(1)–Cu(1)–N(3)	88.8(2)	N(1)–Cu(1)–N(1A)	180.0(1)
N(3)–Cu(1)–N(1A)	91.2(2)	N(1)–Cu(1)–N(3A)	91.2(2)
N(3)–Cu(1)–N(3A)	180.0(1)	N(1A)–Cu(1)–N(3A)	88.8(2)
N(1)–Cu(1)–O(3A)	90.4(2)	N(3)–Cu(1)–O(3A)	91.9(2)
O(1)–Cl(1)–O(2)	112.2(3)	O(1)–Cl(1)–O(3)	108.9(3)
O(2)–Cl(1)–O(3)	108.9(4)	O(1)–Cl(1)–O(4)	109.6(3)
O(2)–Cl(1)–O(4)	108.9(3)	O(3)–Cl(1)–O(4)	108.4(3)
Cu(1)–N(1)–C(1)	129.0(4)	Cu(1)–N(1)–C(4)	125.7(4)
Cu(1A)–O(3)–Cl(1)	163.8(4)	C(1)–N(1)–C(4)	105.0(5)
C(1)–N(2)–C(2)	132.2(6)	C(1)–N(2)–C(3)	106.2(5)
C(2)–N(2)–C(3)	121.6(6)	Cu(1)–N(3)–C(5)	129.8(4)
Cu(1)–N(3)–C(8)	124.6(4)	C(5)–N(3)–C(8)	105.5(5)
C(5)–N(4)–C(6)	131.1(7)	C(5)–N(4)–C(7)	105.2(5)
C(6)–N(4)–C(7)	123.7(7)	N(1)–C(1)–N(2)	109.6(6)
N(2)–C(3)–C(4)	108.2(5)	N(1)–C(4)–C(3)	110.9(5)
N(3)–C(5)–N(4)	110.7(6)	N(4)–C(7)–C(8)	108.4(6)
N(3)–C(8)–C(7)	110.2(5)		

TABLE 3. Atomic coordinates ($\times 10^4$) and equivalent isotropic displacement coefficients ($Å^2 \times 10^3$)

	x	y	z	U_{eq}[a]
Cu(1)	2500	2500	0	31(1)
Cl(1)	699(1)	503(1)	3989(1)	34(1)
O(1)	−121(3)	−84(5)	3431(3)	65(2)
O(2)	1152(4)	1221(6)	3530(3)	82(3)
O(3)	1295(3)	−521(5)	4485(4)	69(2)
O(4)	507(3)	1389(5)	4571(3)	58(2)
N(1)	3511(3)	1174(4)	415(3)	37(2)
N(2)	4816(5)	161(7)	1170(5)	75(3)
N(3)	2386(3)	2404(5)	1160(3)	34(2)
N(4)	2624(4)	2608(7)	2561(3)	62(2)
C(1)	4388(5)	1330(7)	1017(5)	55(3)
C(2)	5755(5)	−248(9)	1773(7)	87(4)
C(3)	4215(4)	−729(5)	667(4)	34(2)
C(4)	3443(5)	−89(7)	219(5)	53(3)
C(5)	2915(5)	2973(7)	1929(4)	41(2)
C(6)	2955(6)	2980(9)	3492(4)	72(3)
C(7)	1892(3)	1800(5)	2170(3)	25(2)
C(8)	1766(4)	1696(6)	1328(4)	41(2)

[a]Equivalent isotropic U defined as one third of the trace of the orthogonalized U_{ij} tensor.

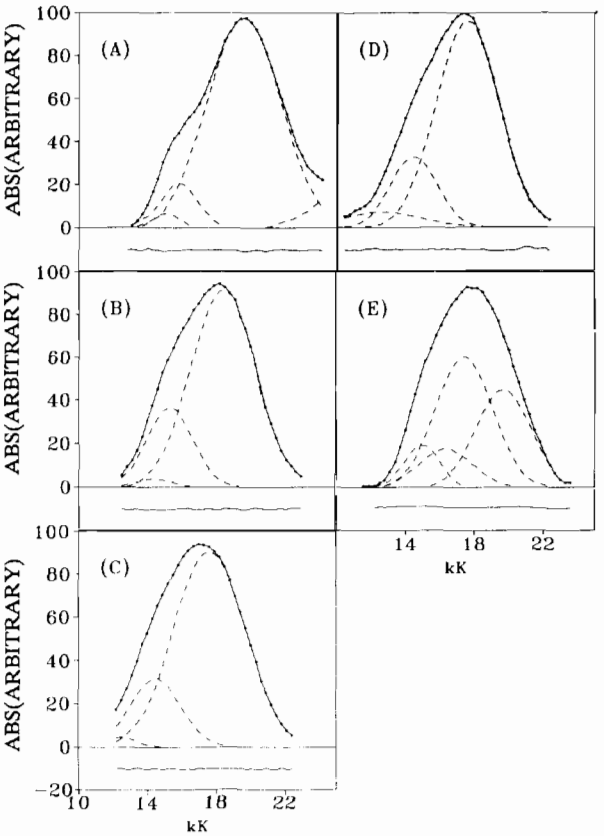

Fig. 3. Solid state visible spectra and Gaussian line-shape analysis with difference plots of (A) $[Cu(4MImH)_4(ClO_4)_2]$, $R = 0.325\%$; (B) $[Cu(4MImH)_4(NO_3)_2]$, $R = 0.580\%$; (C) $[Cu(4MImH)_4Cl_2]$, $R = 0.605\%$; (D) $[Cu(achmH)_4Cl_2]$, $R = 0.532\%$; (E) $[Cu(NMIm)_4(ClO_4)_2]$, $R = 0.577\%$. (——), observed spectrum; (– – –), Gaussian components; (*), profile-fitting points.

mophores have an effective D_{2h} local symmetry, i.e. two imidazole ligands are nearly perpendicular and the other two approximately parallel with respect to the CuN_4 plane, as in the structure of $[Cu(ImH)_4(ClO_4)_2]$ [13]. The ascending of the d_{xz} orbital is a consequence of π-interactions between the copper d_{xz} orbital and the π_2 and π_1 orbitals of the parallel imidazole ligands [14].

The orientation of the coordinated four-substituted imidazole ligands is a reflection of their bonding capabilities, rather than a result due to steric congestion. The steric hindrance involved in both 4-methylimidazole and *N*-methylimidazole complexes is virtually alike, because the coordinated 4-methylimidazole ligand is actually 5-methylimidazole. In fact, the methyl moieties of the coordinated 4-methylimidazole and *N*-methylimidazole produce no hindrance to the adjacent ligands. It is the 2- and 4-hydrogen atoms that give rise to stereochemical problems. Therefore, on the basis of steric effects, these two methylimidazole ligands should behave similarly in coordination as the imidazole ligand does. Indeed, the solid state visible spectra of $[Cu(4MImH)_4(ClO_4)_2]$ and $[Cu(ImH)_4(NO_3)_2]$ are analogous, and so are their structures; the four imidazole rings are approximately perpendicular to the CuN_4 coordination plane. On the other hand, the solid state visible spectrum of $[Cu(NMIm)_4(ClO_4)_2]$ is similar to

TABLE 4. Visible, IR and EPR spectral data for monosubstituted imidazole–copper(II) complexes

Complex[a]	λ_{max} (nm)[b] LF	ν (cm^{-1})[c]		EPR[d]		
		Cu–N	N–H	$g_{\parallel}$	$g_{\perp}$	$A_{\parallel}$[e]
$[Cu(4MImH)_4(ClO_4)_2]$	510 637sh (540)[f]	309m	3362s 3287s.br	2.233	2.053	203
$[Cu(4MImH)_4(NO_3)_2]$	545 650sh (520 600)[f]	305m	3140s	2.243	2.056	194
$[Cu(4MImH)_4Cl_2]$	583 680sh (500 540)[f]	305m	3070s 3050s	~2.379	2.066	
$[Cu(achmH)_4Cl_2]$[g]	570 670sh	291m	3279s	~2.235	2.062	
$[Cu(ImH)_4Cl_2]$	591 700sh (610 725sh)[h]	286m (286s)[i]	3292m 3149s,br (3120s 3060m)[h]	2.160	2.041	
$[Cu(ImH)_4(NO_3)_2]$	(535 650sh)[j]	(291m)[j]	(3243vs,br)[j]			
$[Cu(NMIm)_4(ClO_4)_2]$	563	303m 287mw		2.244	2.053	189
$[Cu(ImH)_4(ClO_4)_2]$	(560)[j]	(310m 283m)[j]	(3356vs,br)[j]			
$[Cu(2MImH)_3(H_2O)_2(ClO_4)_2]$[k]	587	303mw 276m	3188vs 3099vs	[l]		
$[Cu(achmH)_2(NO_3)_2]$[m]	575 700sh	301m	3351s	[n]		
$[Cu(ImH)_2(NO_3)_2]$	(641 741)[o]					

[a]4MImH = 4-methylimidazole; achmH = *N*-acetylhistamine; ImH = imidazole; NMIm = *N*-methylimidazole; 2MImH = 2-methylimidazole. [b]Solid UV–Vis spectra were recorded as Nujol mulls on Whatman No. 1 filter paper; sh = shoulder. [c]Recorded as Nujol mulls or KBr pellets; vs = very strong, s = strong, m = medium, w = weak, br = broad. [d]Powder spectra measured at room temperature. [e]In 10^{-4} cm^{-1}. [f]Ref. 4. [g]Amide I 1665s 1635s cm^{-1}; amide II 1576ms 1545ms cm^{-1}. [h]Ref. 5. [i]Ref. 19. [j]Ref. 3. [k]ν(OH) 3555s 3522s cm^{-1}. [l]Measured at 77 K, g_1 2.004, g_2 2.058, g_3 2.219, $A_{\parallel}$ 155×10^{-4} cm^{-1}. [m]Amide I 1651s cm^{-1}; amide II 1569s cm^{-1}. [n]g_1 2.051, g_2 2.078, g_3 2.274. [o]Ref. 18.

TABLE 5. Gaussian component bands for the visible spectra of tetrakis(monosubstituted imidazole)copper(II) complexes

Band	ν (kK)	ϵ_{max}[a]	$\delta_{1/2}$[b]	Assignments
$[Cu(4MImH)_4(ClO_4)_2]$ (R = 0.325%)[c]				
I	15.1	5	2.3	d_{z^2}
II	15.8	16	2.7	d_{xy}
III	19.6	79	5.0	d_{xz}; d_{yz}
$[Cu(4MImH)_4(NO_3)_2]$ (R = 0.580%)[c]				
I	14.3	3	3.9	d_{z^2}
II	15.3	28	3.2	d_{xy}
III	18.4	69	4.5	d_{xz}; d_{yz}
$[Cu(4MImH)_4Cl_2]$ (R = 0.605%)[c]				
I	12.55	4	3.0	d_{z^2}
II	14.5	25	3.6	d_{xy}
III	17.6	72	5.0	d_{xz}; d_{yz}
$[Cu(achmH)_4Cl_2]$ (R = 0.532%)[c]				
I	12.5	5	6.0	d_{z^2}
II	14.5	24	3.4	d_{xy}
III	17.6	71	4.3	d_{xz}; d_{yz}
$[Cu(NMIm)_4(ClO_4)_2]$ (R = 0.577%)[c]				
I	15.0	14	2.5	d_{z^2}
II	16.4	13	3.85	d_{xy}
III	17.4	42	3.9	d_{xz}
IV	19.7	31	3.8	d_{yz}

[a]Relative band height in arbitrary scale based on a sum of 100. [b]Width at $\epsilon_{max}/2$. [c]R is the reliability factor defined as $R = \Sigma|y_{obs,\,i} - y_{calc,\,i}|/\Sigma y_{obs,\,i}$.

that of $[Cu(ImH)_4(ClO_4)_2]$, of which the structure contains two approximately perpendicular and two parallel imidazoles with respect to the CuN_4 plane.

The structural differences of $[Cu(4MImH)_4(ClO_4)_2]$ and $[Cu(NMIm)_4(ClO_4)_2]$ can be rationalized by the σ-donation abilities of the methylimidazole ligands and the Pauling electroneutrality principle. The σ-donation ability of 4-methylimidazole is stronger than that of both imidazole and *N*-methylimidazole, justified by their pK_a values (imidazole, 6.90 [15]; *N*-methylimidazole, 6.98 [15]; 4-methylimidazole, 7.35 [15]) and also by the energies of their n orbitals (imidazole, −10.17; 4-methylimidazole, −10.06 eV [16]). For the perchlorato complexes, the ClO_4^- anions on the z axis are so weak σ-donors that greater electron density donating from the equatorial ligands to the central copper ion is demanded in order to fulfill the electroneutrality principle. Since 4-methylimidazole ligands with somewhat stronger σ-donating ability may donate enough electron density to the copper ion, no π-interaction is needed. However, π-donation is demanded for both imidazole and *N*-methylimidazole complexes so as to compensate their relatively weak σ-donating capabilities. Moreover, because the copper d_{xz} and d_{yz} orbitals are lower in energy than the d_{xy} orbital in a tetragonal complex and because no *cis* parallel imidazole ligands can accommodate each other, the structure of $[Cu(ImH)_4(ClO_4)_2]$, and presumably $[Cu(NMIm)_4(ClO_4)_2]$ as well, consists of two *trans* imidazole ligands parallel to the CuN_4 plane to facilitate the π-donation to the d_{xz} orbital.

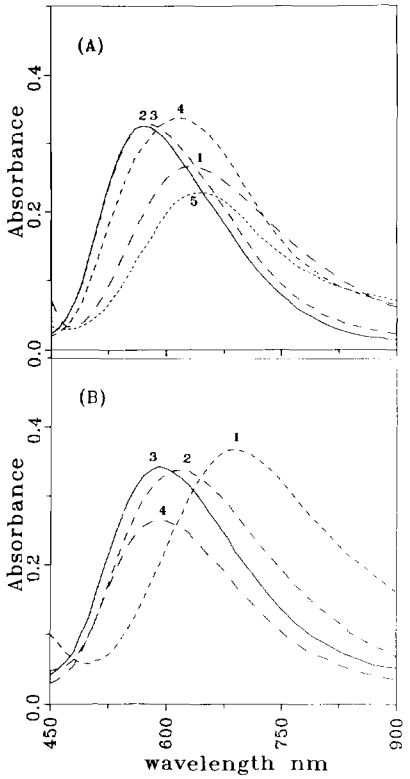

Fig. 4. The LF spectra in CH_3CN of: (A) Cu(II)–4-methylimidazole complex with [4MImH]/[Cu^{2+}] at (1) 2, (2) 4, (3) 5, (4) 10, (5) 100* and [Cu^{2+}]=4.94 mM, *[Cu^{2+}]=3.12 mM; (B) Cu(II)–*N*-acetylhistamine complex with [achmH]/[Cu^{2+}] at (1) 2, (2) 3, (3) 4, (4) Saturated achmH and [Cu^{2+}]=4.94 mM.

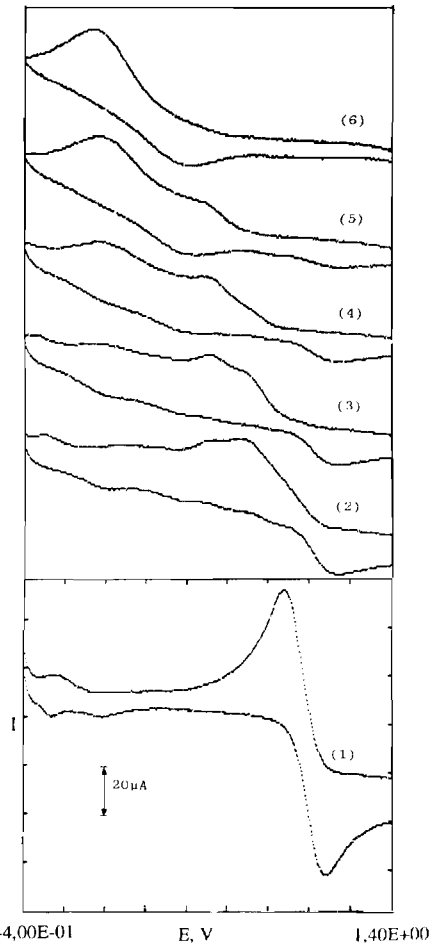

Fig. 5. Cyclic voltammetry profiles of 2.19 mM $Cu(BF_4)_2$ in CH_3CN containing (1) 0; (2) 2.19; (3) 4.38; (4) 6.57; (5) 8.76; and (6) 10.9 mM of 4-methylimidazole. 0.1 M $N(Et)_4(BF_4)$; scan rate 0.1 V s^{-1}; Pt working electrode vs. SCE.

Since the donor ability of chloride ions is better than that of ClO_4^-, no π-donation from the imidazole ligands is needed for the chloro complexes. Based on their solid state visible spectra, all of the chloro complexes belong to the first group with effective D_{4h} symmetry, namely, none of the coordinated imidazole ligands lies parallel to the CuN_4 plane.

In line with this context, one would expect the complexes of *N*-acetylhistamine (pK_a 7.1 [17]) to be similar to those of imidazole, and the complexes of 2-methylimidazole (pK_a 7.77 [15]) to be similar to those of 4-methylimidazole. Our results suggest that $[Cu(achmH)_4Cl_2]$ is similar to $[Cu(ImH)_4Cl_2]$ [5] and $[Cu(achmH)_2(NO_3)_2]$ is similar to $[Cu(ImH)_2(NO_3)_2]$ [18]. Attempts to prepare $[Cu(achmH)_4(ClO_4)_2]$, which would be similar to $[Cu(ImH)_4(ClO_4)_2]$, were unsuccessful. This may be attributed to the bulky substituent on achmH preventing the imidazole nuclei of the achmH ligands from lying parallel to the CuN_4 coordination plane. For 2-methylimidazole, $[Cu(2MImH)_4Cl_2]$ has been isolated [19]. However, the perchlorate complex we isolated contains only three 2MImH ligands, perhaps, due to steric congestion [20].

The rhombic EPR spectrum for $[Cu(achmH)_2(NO_3)_2]$ suggests a six-coordinated structure with NO_3^- as bidentate ligands. All of the tetrakis complexes show the expected axial EPR spectra.

The designation of Cu–N stretchings of the mono-substituted imidazole complexes was complicated by the presence of ligand peaks in the far-IR region. The peaks were assigned based on the following considerations: (i) there should be only one ν(Cu–N) for the first group complexes with D_{4h} local symmetry and two for the second group with D_{2h} local symmetry; and (ii) the peak should appear in the vicinity of ν(Cu–N) of the imidazole complexes, namely, ~300 cm^{-1} [21], because the Cu–N bond lengths are essentially unvaried for the tetra-coordinated complexes of known structures. Red shifts of the imidazole N–H stretchings of the complexes were observed, indicating hydrogen bonds in the complexes. The amide I and II peaks are not much varied upon formation of the achmH complexes,

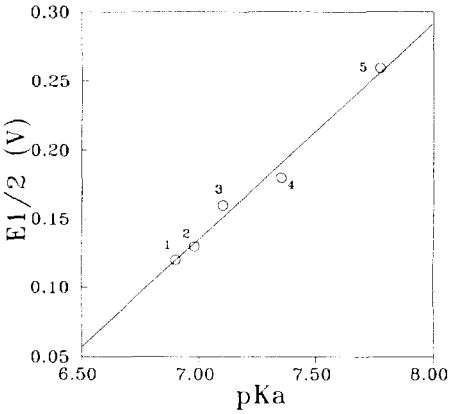

Fig. 6. Plot of $E_{1/2}$ of tetrakis(imidazole)copper(II) complexes vs. pK_a of imidazole ligands: 1, imidazole; 2, *N*-methylimidazole; 3, *N*-acetylhistamine; 4, 4-methylimidazole; 5, 2-methylimidazole.

suggesting that the amide oxygen does not coordinate to the central metal in these complexes.

It is intriguing to investigate the copper imidazole complexes in solution. In order to ensure the species in acetonitrile, the visible and EPR spectra of the imidazole copper complexes with different imidazole:copper ratios were recorded. As illustrated in Fig. 4, the LF band maxima of these complexes blue-shifted to the highest frequency limit shown in Table 6 with the ratio of ~5. For 4-methylimidazole, *N*-methylimidazole and imidazole complexes, the LF band maxima red-shifted gradually to low energy region as the ligand:copper ratio was further increased, indicating that species comprising more than four imidazole ligands are easily formed in CH_3CN when the ligand to copper ratio is greater than five-fold, in contrast to the coordination behavior in aqueous systems [22, 23]. For 2-methylimidazole and *N*-acetylhistamine, no red shift was observed while keeping the ratio greater than 5, suggesting that the number of coordinated imidazole ligands cannot be increased, apparently, due to steric hindrance.

For each of the complexes having a ligand:copper ratio of 5, the solution EPR spectra measured at 77 K are of the axial type having $g_{\parallel} > g_{\perp} > 2$ [24], consistent with the presence of the species having square planar CuN_4 units. The spectra became complicated at room temperature, due to free tumbling of the molecules. For solutions with a ligand:copper ratio of 100, complexes containing six imidazole ligands can be suggested from their EPR spectra, where the *N*-superhyperfine lines were observed. The *G* values are larger than 4, indicating negligible exchange coupling for the complexes in CH_3CN [25]. Since the tetrakis complexes are completely ionized in acetonitrile, as suggested from their high conductivity values, the axial ligands are replaced by CH_3CN molecules. The λ_{max} values of the tetrakis complexes in CH_3CN vary only slightly, reflecting that the ligand field strengths of the imidazole ligands are similar in the copper(II) complexes.

The cyclic voltammograms of 4-methylimidazole copper(II) complexes in acetonitrile, shown in Fig. 5, are typical of imidazole copper(II) complexes studied here. As successive amounts of ligands were added to the Cu(II) solution, a series of cathodic and anodic peaks with decreasing reduction potentials, corresponding to copper complexes having different numbers of coordinated imidazole ligands, were observed. The electrochemical data for the monosubstituted imidazole copper(II) complexes having the ligand:copper ratio of

TABLE 6. Visible and EPR spectral data for monosubstituted imidazole copper(II) complexes in CH_3CN[a]

System ligand:Cu(II)	$g_{\parallel}$	$A_{\parallel}$[b]	$g_{\perp}$	$A_{\perp}$ (N)[b]	G[c]	λ_{max} (nm) (ϵ)
4-Methylimidazole						
5:1	2.248	194	2.049		5.06	573(65)
100:1	2.259	176	2.055	15	4.71	642(46)
N-Methylimidazole						
5:1	2.260	185	2.057		4.56	578(52)
100:1	2.266	180	2.056	14	4.75	645(44)
Imidazole						
5:1	2.250	189	2.058		4.31	576(50)
100:1	2.261	179	2.054	14	4.83	642(42)
2-Methylimidazole						
5:1	2.235	198	2.047		5.00	571(81)
N-Acetylhistamine						
4:1	2.244	194	2.050		4.88	585(69)

[a]EPR spectra measured at 77 K. [b]In 10^{-4} cm^{-1}. [c]$G = (g_{\parallel} - 2)/(g_{\perp} - 2)$.

TABLE 7. Electrochemical data for monosubstituted imidazole copper(II) complexes in CH_3CN[a]

System ligand:Cu(II)	Scan rate[b]	$E_{p,c}$	$E_{p,a}$	ΔE_p	$E_{1/2}$	$i_{p,a}/i_{p,c}$
4-Methylimidazole[c]						
5.0:1	0.05	0.05	0.30	0.25	0.18	0.74
	0.10	0.03	0.32	0.29		0.70
	0.50	−0.04	0.39	0.43		0.65
N-Methylimidazole[d]						
5.0:1	0.05	0.01	0.23	0.24	0.13	0.84
	0.10	−0.01	0.27	0.28		0.79
	0.50	−0.07	0.32	0.39		0.76
Imidazole[e]						
5.0:1	0.05	0.00	0.23	0.23	0.12	0.80
	0.10	−0.03	0.26	0.29		0.77
	0.50	−0.11	0.33	0.44		0.73
2-Methylimidazole[f]						
5.0:1	0.05	0.07	0.40	0.33	0.26	0.73
	0.10	0.06	0.44	0.50		0.67
	0.50	−0.01	0.54	0.55		0.64
N-Acetylhistamine[g]						
5.0:1	0.05	−0.01	0.34	0.35	0.16	0.73
	0.10	−0.04	0.39	0.43		0.69
	0.50	−0.16	0.47	0.63		0.58

[a]All potentials were reported as V vs. SCE. Acetonitrile containing 1% 2,2-dimethoxypropane. [b]V/s. [c]$[Cu^{2+}]=4.51$ mM. [d]$[Cu^{2+}]=6.84$ mM. [e]$[Cu^{2+}]=9.36$ mM. [f]$[Cu^{2+}]=6.19$ mM. [g]$[Cu^{2+}]=5.33$ mM.

~5 are collected in Table 7. The separation of the cathodic and anodic peaks of the quasi-reversible voltammograms decreased as the scan rates were reduced. The peak–current ratio, $i_{p,a}/i_{p,c}$, decreases from a value of ~0.8 at a scan rate of 50 mV/s to smaller values at higher scan rates and is consistent with a reversible chemical reaction following the first one-electron addition [26].

The reduction potentials of the four-coordinated complexes increase with increase of the pK_a values of the ligands. This relationship is illustrated by the linear plot of the $E_{1/2}$ value versus the free ligand pK_a in Fig. 6. The linear plot with a positive slope is in contrast to the results reported for the pyrrole-2-carboxaldiminate copper(II) complexes [27], and the 1,10-phenanthroline and 2,2′-bipyridine copper(II) complexes [28]. Since the λ_{max} values of the d–d band for the tetrakis imidazole copper(II) complexes are nearly alike, the Cu(II)/Cu(I) redox change in the 2-methylimidazole complex at a markedly more positive potential (more than 100 mV) than for the imidazole complex, suggests that the Cu(I) complexes are greatly stabilized by strong σ-donor ligands. This situation is in contrast to the tetraaza macrocyclic copper complexes [29]. It is likely that the copper(I) complexes here are two-coordinate [30], and can be stabilized through σ-donation, while the tetraaza macrocyclic copper(I) complexes are stabilized via π-accepting processes.

Conclusions

We have demonstrated that the orientation of the coordinated imidazole nuclei and consequently the geometry of the copper(II) complexes are affected by the σ-donor abilities of the axial ligands and the bonding capabilities and steric effects of the equatorial imidazole ligands. The bulky 4-substituent of the *N*-acetylhistamine may exert profound steric effects upon complexing with copper ions if the counter ions are very weak σ-donors, and the stereochemistry will be greatly affected. We anticipate that the copper complex containing two *N*-acetylhistamine ligands has high reduction potential. Unfortunately, we were not able to measure the reduction potential for this species due to the participation of the solvent molecules in the coordination sphere in solution. A study of copper(II) complexes utilizing imidazole ligands with a bulky 4-substituent to lower the coordination number should be useful in elucidating the properties of the Cu–histidyl residue bonding in copper proteins, and is currently in progress.

Supplementary material

Additional material comprising structure factors, anisotropic thermal parameters and H atom coordinates are available from the authors on request.

Acknowledgements

We thank Professor K. H. Lii for use of his computer facilities and the National Science Council of the Republic of China for financial support (NSC79-0208-M-003-02).

References

1 T. G. Spiro (ed.), *Copper Proteins,* Wiley, New York, 1981.
2 R. J. Sundberg and R. B. Martin, *Chem. Rev., 74* (1974) 471.
3 C.-C. Su, T.-T. Hwang, O. Y.-P. Wang, S.-L. Wang and F.-L. Liao, *Transition Met. Chem., 17* (1992) 91.
4 K. C. Dash and C. K. C. Mohapatra, *Transition Met. Chem., 2* (1977) 155.
5 W. J. Eilbeck, F. Holmes and A. E. Underhill, *J. Chem. Soc., A,* (1967) 757.
6 S.-L. Wang, P. C. Wang and Y. P. Nieh, *J. Appl. Crystallogr., 23* (1990) 520.
7 G. M. Sheldrick, *SHELXTL PLUS User Manual,* Nicolet XRD Corporation, Madison, WI, 1986.
8 *International Tables for X-ray Crystallography,* Vol. 4, Kynoch, Birmingham, UK, 1974.
9 I. Olovsson and P.-G. Jonsson, in P. Schuster, G. Zundel and C. Sandorfy (eds.), *The Hydrogen Bond,* Vol. II, North-Holland, Amsterdam, 1976, pp. 393–456.
10 D. L. McFadden, A. T. McPhail, C. D. Garner and F. E. Mabbs, *J. Chem. Soc., Dalton Trans.,* (1975) 263.
11 B. J. Hathaway and A. A. G. Tomlinson, *Coord. Chem. Rev., 5* (1970) 1.
12 D. L. McFadden, A. T. McPhail, C. D. Garner and F. E. Mabbs, *J. Chem. Soc., Dalton Trans.,* (1976) 47.
13 G. Ivarsson, *Acta Chem. Scand., 27* (1973) 3523.
14 T. G. Fawcett, E. E. Bernarducci, K. Krogh-Jespersen and H. J. Schugar, *J. Am. Chem. Soc., 102* (1980) 2598.
15 F. Jiang, J. McCracken and J. Peisach, *J. Am. Chem. Soc., 112* (1990) 9035.
16 E. Bernarducci, P. K. Bharadwaj, K. Krogh-Jespersen, J. A. Potenza and H. J. Schugar, *J. Am. Chem. Soc., 105* (1983) 3860.
17 P. M. H. Kroneck, V. Vortisch and P. Hemmerich, *Eur. J. Biochem., 109* (1980) 603.
18 D. M. L. Goodgame, M. Goodgame, P. J. Hayward and G. W. Rayner-Canham, *Inorg. Chem., 7* (1968) 2447.
19 W. J. Eilbeck, F. Holmes, C. E. Taylor and A. E. Underhill, *J. Chem. Soc. A,* (1968) 128.
20 A. R. Rossi and R. Hoffmann, *Inorg. Chem., 14* (1975) 365.
21 J. B. Hodgson, G. C. Percy and D. A. Thornton, *J. Mol. Struct., 66* (1980) 81.
22 R. P. Bonomo, F. Riggi and A. J. Di Bilio, *Inorg. Chem., 27* (1988) 2510.
23 S. Siddiqui and R. E. Shepherd, *Inorg. Chem., 25* (1986) 3869.
24 B. J. Hathaway, *J. Chem. Soc., Dalton Trans.,* (1972) 1196.
25 B. J. Hathaway and D. E. Billing, *Coord. Chem. Rev., 5* (1970) 143.
26 R. S. Nicholson and I. Shain, *Anal. Chem., 36* (1964) 706.
27 A. W. Addison and J. H. Stenhouse, *Inorg. Chem., 17* (1978) 2161.
28 B. R. James and R. J. P. Williams, *J. Chem. Soc.,* (1961) 2007.
29 L. Fabbrizzi, A. Lari, A. Poggi and B. Seghi, *Inorg. Chem., 21* (1982) 2083.
30 T. N. Sorrell and D. L. Jameson, *J. Am. Chem. Soc., 105* (1983) 6013.